Boltzmann Machine Using Superconducting Circuits

Kohei Miyake, Yuki Yamanashi, *Member, IEEE,* and Nobuyuki Yoshikawa, *Senior Member, IEEE*

***Abstract*—We study the design and optimization of the Boltzmann machine hardware using superconducting circuits as a new stochastic information processing method. The Boltzmann machine is an artificial neural network of stochastic binary models wherein the energy function is determined by the given set of parameters, and the output is obtained by stochastic state transitions of the system to the energy stable states according to the Boltzmann distribution. By adjusting the set of parameters, arbitrary functions can be embedded in energy-stable states, which have applications in data dimensionality reduction and generative models. The hardware of a Boltzmann machine using superconducting circuits consists of quantum flux parametrons (QFPs), one of the superconducting circuits, magnetically coupled to each other. In this study, we designed the Boltzmann machine hardware in which logic gates such as NOR are embedded in energy-stable states. Furthermore, we applied maximum likelihood estimation (MLE), machine learning method, as an operating-point optimization method, and confirmed the effectiveness of this method in experiments.**

***Index Terms*—Superconducting circuits, Quantum flux parametron (QFP), Artificial neural networks (ANN), Boltzmann machine, Optimization, Maximum likelihood estimation (MLE)**

I. Introduction

NEUROMORPHIC computing is an approach to create an artificial neural network (ANN) in hardware that mimics the function of the biological brain [1]. By implementing ANNs based on specialized hardware, information can be processed at higher speeds and with lower power consumption [2]. In addition, this approach is attracting attention as a way to overcome the limitation of the von Neumann bottleneck between the processor and memory [3]. Neuromorphic computing using semiconductor circuits has already been realized, and it has been confirmed that the operating speed is improved in comparison with that obtained by software-based implementations [4], [5], [6]. However, semiconductor integrated circuits are approaching their physical limitations [7] and cause an increase in the leakage current [8]; moreover, an increase in power consumption is a concern when realizing large-scale circuits such as ANNs [9]. Therefore, the implementation using superconducting circuits has been attracting attention as a method of hardware implementation of ANNs with lower power consumption [10], [11], [12], [13], [14], [15].

A Boltzmann machine is stochastic ANN consisting of neurons of a stochastic binary model coupled with each other [16]. For a given set of parameters, the energy function of the entire system of the network is uniquely determined, and the output is obtained by the stochastic transition of the state of the entire system to one of its energy-stable states. By adjusting the set of parameters, arbitrary functions can be enabled in energy-stable states [17], and the typically used parameter adjustment method based on statistical machine learning is maximum likelihood estimation (MLE). Therefore, the Boltzmann machine can preserve arbitrary functions as a set of parameters, and can be applied to data dimensionality reduction and generative models [18]. In addition, several new information processing methods have been proposed by applying stochastic state transitions based on the energy functions of Boltzmann machines [19], [20]. Furthermore, attempts to apply quantum annealing machines as samplers of Boltzmann machines that follow the Boltzmann distribution have been proposed [21], [22], [23].

In our study, as one of the hardware implementations of ANNs using superconducting circuits, we investigated the Boltzmann machine hardware using quantum flux parametrons (QFPs), by magnetically coupling QFPs with each other [24]. A QFP is an energy-efficient superconducting circuit that is noted as a future technology for building an energy-efficient computing system because a significant reduction in the power consumption can be enabled using AC adiabatic biasing [25].

In Boltzmann machine hardware, it is important to correctly optimize the set of parameters of the hardware corresponding to the set of parameters in the mathematical model of the Boltzmann machine. In experiments, fine optimization is required to drive the optimal set of parameters due to the unintended external noise and manufacturing variation. As an optimization method for the set of parameters of Boltzmann machine hardware, we applied MLE and confirmed that logic gates such as NOR were correctly embedded in the energy-stable states. This optimization process can be referred to as closed-loop optimization consisting of a superconducting circuit that operates at cryogenic temperatures and the statistical machine learning framework at room temperatures [26]. In the remainder of this paper, Section II describes the Boltzmann machine hardware using QFPs, Section III describes the experimental results, and Section IV presents the conclusions.

II. Boltzmann Machine Hardware

A. Mathematical Model of Boltzmann Machines

A Boltzmann machine is stochastic ANN consisting of neurons coupled with each other [16]. Fig. 1 shows a Boltzmann machine consisting of three neurons, where x_i represents the state of the i-th neuron as a binary value of "-1" or "$+1$" corresponding to logic states, "0" and "1", respectively, and the state of the entire system is represented by the vector $\boldsymbol{x}$

This work was supported by JSPS KAKENHI Grant Number JP18K04280 and JP19H05614.

K. Miyake, Y. Yamanashi, and N. Yoshikawa are with Department of Electrical and Computer Engineering, Yokohama National University, Yokohama 240-8501, Japan (e-mail: yamanashi-yuki-kr@ynu.ac.jp).

Color versions of one or more of the figures in this paper are available online at http://ieeexplore.ieee.org.

Digital Object Identifier will be inserted here upon acceptance.

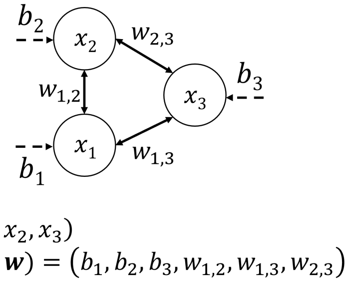

Fig. 1. Boltzmann machine consisting of three neurons, where x_i ($\in$ {0,1}) represents the state of the i-th node, vector $\boldsymbol{x}$ represents the state of the entire system, b_i is the bias energy of the i-th neuron (collectively described as vector $\boldsymbol{b}$ for all neurons), and $w_{i,j}$ is the coupling energy between the i-th and j-th (collectively described as vector $\boldsymbol{w}$). The vectors $\boldsymbol{b}$ and $\boldsymbol{w}$ are collectively called the set of parameters $\boldsymbol{\theta}$ of the Boltzmann machine.

= (x_1, x_2, x_3). In addition, b_i denotes the bias energy of the i-th neuron, which are collectively described as vector $\boldsymbol{b}$ for all neurons, and $w_{i,j}$ denotes the coupling energy between the i-th and j-th neurons which are collectively described as vector $\boldsymbol{w}$ for all couplings between all neurons. The vectors $\boldsymbol{b}$ and $\boldsymbol{w}$ are collectively called the set of parameters $\boldsymbol{\theta}$ of the Boltzmann machine. For a given $\boldsymbol{\theta}$, the probability distribution of the single i-th neuron, which is a stochastic binary model, is defined by

$$P(x_i = 1|\boldsymbol{\theta}) = \sigma\left(b_i + \sum_j w_{i,j}x_j\right), \tag{1a}$$

$$P(x_i = -1|\boldsymbol{\theta}) = 1 - P(x_i = 1|\boldsymbol{\theta}), \tag{1b}$$

where $\sigma(x)$ is the sigmoid function = 1/(1+exp($-x$)), and $\sum_j w_{i,j}x_j$ is the sum of all neurons that connect to the i-th neuron. The neurons recursively influence each other to determine the state $\boldsymbol{x}$.

The energy function of the entire system of the Boltzmann machine consisting of N neurons is defined as

$$E(\boldsymbol{x}|\boldsymbol{\theta}) = -\sum_i^N b_i x_i - \sum_{j>i}^N \sum_i^N w_{i,j}x_i x_j. \tag{2}$$

The state $\boldsymbol{x}$, in which the energy function is minimized for the given $\boldsymbol{\theta}$, is the energy stable state of the Boltzmann machine. Therefore, by adjusting $\boldsymbol{\theta}$ correctly, it is possible to embed logic gates in the energy-stable states [17], [19], [24]. For example, the NOR is realized by a Boltzmann machine consisting of three neurons when $\boldsymbol{b}$ = (b_1, b_2, b_3)=(-1, -1, -2), $\boldsymbol{w}$ = ($w_{1,2}$, $w_{1,3}$, $w_{2,3}$)=(-1, -2, -2). For these parameters, Equation (2) yields the minimum value of E($\boldsymbol{x}|\boldsymbol{\theta}$) = -3 when the energy stable states satisfy the NOR operation, that is, $\boldsymbol{x}$ = (-1, -1, 1), (-1, 1, -1), (1, -1, -1), (1, 1, -1), assuming that the inputs at the logic gate are x_1, x_2 and the output is x_3. In all other states, E($\boldsymbol{x}|\boldsymbol{\theta}$) > -3.

B. Boltzmann Machine Using QFP

Fig. 2(a) shows the schematic of a QFP where J_1 and J_2 are Josephson junctions (JJs) with critical current I_C = 50 μA, and L_1, L_2, and L_q represent the inductances of 2.33 pH, 2.33 pH, and 14.4 pH, respectively. The device parameters were based on the 10 kA/cm^2 Nb high-speed standard process (HSTP) of the National Institute of Advanced Industrial Science and Technology (AIST) [27]. The QFP consists of two superconducting loops, an inner loop consisting of J_1, J_2, L_1 and L_2, and a main loop consisting of a pair of JJs and L_q. When the quantum flux $\Phi_0 \approx 2.07 \times 10^{-15}$ Wb is applied to the inner loop by the excitation current I_x, the potential of QFP changes from single-well to double-well, and a current I_q flows in the main loop to satisfy the flux quantization. The direction of the current I_q corresponds to the logical state q as the binary value of "0" or "1", and the transition to either state is determined by the weak input magnetic flux Φ_b by the bias current I_b to the main loop and thermal fluctuations. Fig. 2(b) shows the JSIM [28] simulation result of the probability distribution of the state of the QFP in Fig. 2(a) for the current I_b, and it can be confirmed that the fitting can be achieved with P(I_b) = $\sigma(-0.112 I_b)$. Therefore, the QFP can be applied to the Boltzmann machine as a neuron of a stochastic binary model. In the simulation, thermal noise current is added to J_1 and J_2 in parallel assuming the operation temperature T = 4.2 K [29].

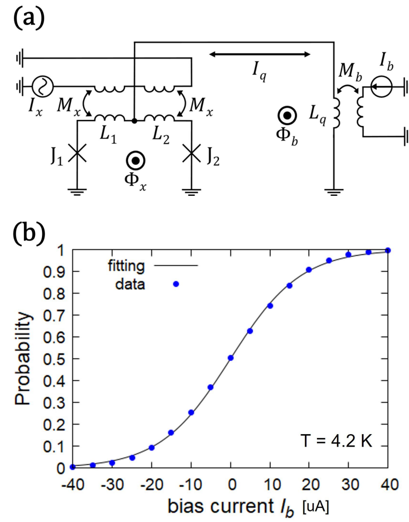

Fig. 2. (a) Schematic of QFP where J_1 and J_2 are Josephson junctions with critical current I_C = 50 μA, I_x is the excitation current, and I_b is the bias current. The circuit parameters are L_1 = L_2 = 2.33 pH, L_q = 14.4 pH, M_x = -0.75 pH, and M_b = 1.21 pH. (b)Probability distribution of the state of QFP for the bias current I_b. It can be fitted with P(I_b) = 1/(1+exp($-0.112 I_b$)) by the sigmoid function.

Fig. 3 shows the Boltzmann machine hardware consisting of the three QFPs, namely Q1, Q2 and Q3, as shown in Fig. 2(a). The bias current $\boldsymbol{I_b}$ and the mutual inductance $\boldsymbol{M}$ in the hardware shown in Fig. 3 correspond to the bias energy $\boldsymbol{b}$ and the coupling energy $\boldsymbol{w}$ in the mathematical model shown in Fig. 1, respectively. The state of the Boltzmann machine hardware is determined by the direction of the current flowing in the main loop of each QFP when all QFPs are excited at once by the excitation current I_x, as shown in Fig. 4. By repeating this sequence, the probability distribution for all states is obtained.

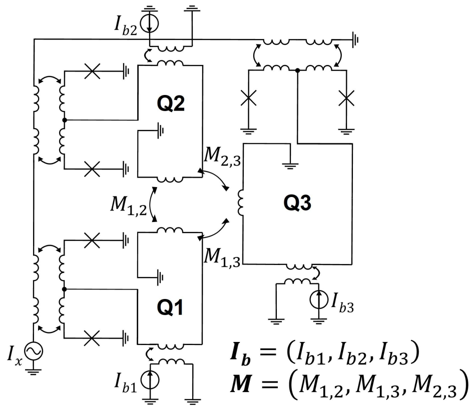

Fig. 3. Boltzmann machine hardware consisting of three neurons using QFPs. The bias current $\boldsymbol{I_b}$ and mutual inductance $\boldsymbol{M}$ correspond to the bias energy $\boldsymbol{b}$ and coupling energy $\boldsymbol{w}$, respectively.

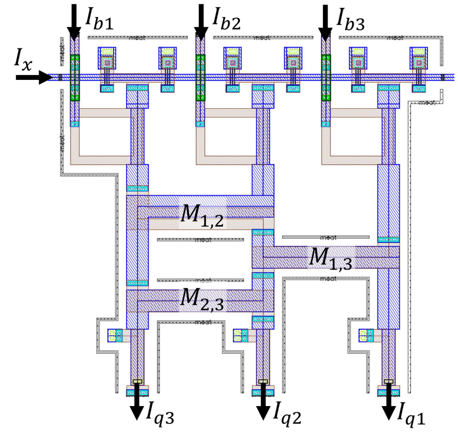

Fig. 5. Layout of Boltzmann machine hardware designed to embed NOR.

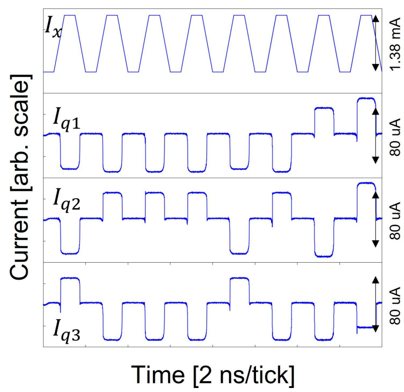

Fig. 4. Example of the output of the Boltzmann machine hardware. The state is determined by the direction of currents I_{q1}, I_{q2}, and I_{q3}.

To embed functions such as NOR in the energy-stable states of the Boltzmann machine hardware, the adjustments of $\boldsymbol{I_b}$ and $\boldsymbol{M}$ corresponding to $\boldsymbol{b}$ and $\boldsymbol{w}$ are required. Fig. 5 shows the layout of the Boltzmann machine hardware designed to embed NOR. The $\boldsymbol{M}$ corresponding to $\boldsymbol{w}$ was designed with $\boldsymbol{M}$ = ($M_{1,2}$, $M_{1,3}$, $M_{2,3}$) = (-0.89 pH, -1.78 pH, -1.77 pH) to satisfy the relationship illustrated in the previous section. These parameters were extracted using a 3D inductance extractor, InductEx [30]. While the mutual inductance $\boldsymbol{M}$ is the parameter determined by the layout design, the bias current $\boldsymbol{I_b}$ is the parameter applied from the outside in the experiment. The optimum bias current $\boldsymbol{I_b}$ differs between experiments and simulations due to the unintended external noise and manufacturing variation. To optimize the bias current, we applied MLE, statistical machine learning method.

III. Experiment

A. Optimization Algorithm

For the Boltzmann machine, learning means learning the set of parameters that reproduce the probability distribution of arbitrary data, applying MLE. This is the minimization of the Kullback-Leibler divergence [31] between the probability distribution of arbitrary data and that generated by the Boltzmann machine.

Considering the design of the NOR in the Boltzmann machine hardware, MLE can optimize the set of parameters $\boldsymbol{I_b}$ to reproduce the probability distribution of the NOR operation. **Algorithm 1** shows the optimization algorithm based on MLE applied to the Boltzmann machine hardware. The update rule for the set of parameters $\boldsymbol{I_b}$ is

$$I_{bi}^{\mathrm{new}} \leftarrow I_{bi}^{\mathrm{old}} + \epsilon(E_{\mathrm{NOR}}[x_i] - E_{\mathrm{samp}}[q_i|\boldsymbol{I_b}, \boldsymbol{M}]), \qquad (3)$$

where E_{NOR} $[x_i]$ is the expected value of the state of the i-th neurons in the NOR; E_{samp} $[q_i|\boldsymbol{I_b}$, $\boldsymbol{M}]$ is the expected value of the state of the i-th QFP obtained by sampling any number of times from the Boltzmann machine hardware, given the parameters $\boldsymbol{I_b}$ and $\boldsymbol{M}$; and ϵ is the learning rate for determining the magnitude of the update. Obtaining a large number of samples requires a lot of time. Therefore, in the optimization algorithm, the number of samplings was small and the learning rate was large for the coarse optimization in the initial stage; in contract, the number of samplings was large and the learning rate was small for the fine optimization in the final stage.

Algorithm 1 $\boldsymbol{I_b}$ Optimization Based on MLE

Input: Expected value of NOR $\boldsymbol{E}_{\mathbf{NOR}}$
Output: Optimal bias current $\boldsymbol{I_b}$

```
    Initialization :
stage = 0
s = [100, 500, 1000]
ε = [0.02, 0.01, 0.005]
    LOOP Process
while do
    sampling s[stage] times to get the E_samp
    I_b^new ← I_b^old +ε[stage](E_NOR - E_samp)
    if ||E_NOR - E_samp|| < 0.2/(2^stage) then
        stage += 1
        if stage > 3 then
            break
        end if
    end if
end while
```

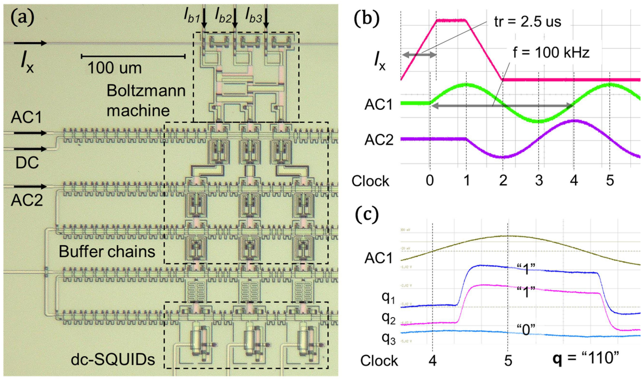

Fig. 6. (a) Photomicrograph of the Boltzmann machine hardware fabricated using HSTP. (b) Sequence of excitation currents for the Boltzmann machine, buffer chains, and dc-SQUIDs. (c) Example of the output waveforms, where the state $\boldsymbol{q}$ = "110" is read.

B. Measurement System

Fig. 6(a) shows a photomicrograph of the Boltzmann machine hardware fabricated using HSTP. A test chip is placed inside a dipping probe and is immersed in liquid He (at 4.2 K). Fig. 6(b) shows the sequence of excitation currents for the Boltzmann machine, buffer chains, and dc-SQUIDs. The rise time of the excitation current I_x was set to t_r = 2.5 μs. The state of the Boltzmann machine hardware determined by I_x was propagated by buffer chains at clock "1" that were powered and clocked by a pair of sinusoidal excitation currents of 100 kHz, AC1 and AC2 [27], and then read by dc-SQUIDs at clock "5". Fig. 6(c) shows an example of the output waveforms, where the state $\boldsymbol{q}$ = "110" is read.

C. Experimental Results

Fig. 7 depicts the probability distributions obtained by sampling 1000 times at specific bias values, respectively. Fig. 7(a) shows the probability distribution at $\boldsymbol{I_b}$ = (0 μA, 0 μA, 0 μA) before the optimization, and Fig. 7(b) shows the probability distribution at $\boldsymbol{I_b}$ = (-81 μA, -83 μA, -88 μA) after the optimization shown in **Algorithm 1**. The probability distribution after the optimization satisfies the NOR operation that the four states $\boldsymbol{q}$ = "001", "010", "100", "110" are obtained with equally high probability. Therefore, it can be said that the bias currents $\boldsymbol{I_b}$ were correctly optimized by **Algorithm 1**. Fig. 7(c) and (d) depicts the results when I_{b3} was varied positively and negatively by 20 μA as the inverse operation [19], [24] respectively. Based on these results, it can be said that the inverse operations of NOR were realized. Fig. 8 shows the error rate obtained by sampling 1000 times when the rise time t_r was varied at $\boldsymbol{I_b}$ = (-81 μA, -83 μA, -88 μA), for the case where logic states other than NOR are read as an error. From this result, it can be said that the rise time should be more than 1 μs for the designed Boltzmann machine hardware.

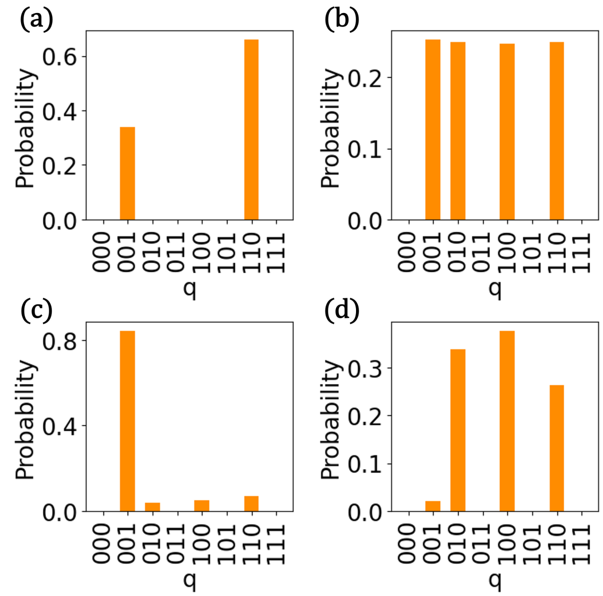

Fig. 7. Probability distributions obtained by sampling 1000 times. (a) $\boldsymbol{I_b}$ = (0.0 μA, 0.0 μA, 0.0 μA) (b) $\boldsymbol{I_b}$ = (-81 μA, -83 μA, -88 μA) (c) $\boldsymbol{I_b}$ = (-81 μA, -83 μA, -68 μA) (d) $\boldsymbol{I_b}$ = (-81 μA, -83 μA, -108 μA).

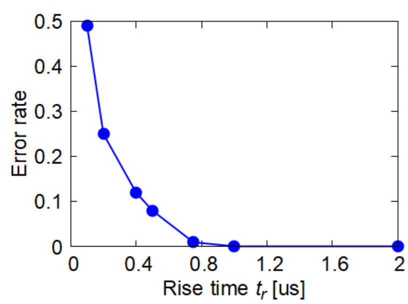

Fig. 8. Error rate obtained by sampling 1000 times when the rise time t_r is varied at $\boldsymbol{I_b}$ = (-81 μA, -83 μA, -88 μA).

IV. Conclusion

We designed a Boltzmann machine hardware as a novel stochastic information processing method using superconducting circuits. In addition, we proposed a method for optimizing the bias currents by applying MLE and confirmed that the bias currents were correctly optimized in the designed Boltzmann machine hardware that embedded NOR operation. Furthermore, the inverse operation was realized in the designed NOR by varying the current corresponding to the output from the optimum bias value to positive or negative.

These results suggest that the basic elements constituting the stochastic ANNs can be efficiently designed by applying these design and optimization methods. In the future, it will be necessary to optimize the design of device parameters in order to improve the operation speed.

Acknowledgment

The circuits were fabricated in the clean room for analog-digital superconductivity (CRAVITY) of National Institute of Advanced Industrial Science and Technology (AIST) with the high-speed standard process (HSTP).

References

[1] D. Markovic, A. Mizrahi, D. Querlioz, and J. Grollier, "Physics for neuromorphic computing," *Nat. Rev. Phys.*, vol. 2, pp. 499-510, Jul. 2020.

[2] C. S. Poon and K. Zhou, "Neuromorphic silicon neurons and largescale neural networks: challenges and opportunities," *Front. Neurosci.*, vol. 5, no. 22, Sep. 2011.

[3] J. Backus, "Can programming be liberated from the von Neumann style? A functional style and its algebra of programs," *Commun. ACM*, vol. 21, pp. 613-641, Aug. 1978.

[4] H. Tanaka, T. Morie, and K. Aihara, "An analog CMOS circuit for spiking neuron models," *Int. Congr. Ser.*, vol. 1291, pp. 217–220, Jun. 2006.

[5] I. Sourikopoulos, S. Hedayat, C. Loyez, F. Danneville, V. Hoel, E. Mercier, and A. Cappy, "A 4-fJ/Spike artificial neuron in 65 nm CMOS technology," *Front. Neurosci.*, vol. 11, no. 123, Mar. 2017.

[6] Y. Du, L. Du, X. Gu, J. Du, X. S. Shawn, B. Hu, M. Jiang, X. Chen, S. S. Iyer, M. F. Chang, "An analog neural network computing engine using CMOS-compatible charge-trap-transistor (CTT)," *IEEE Trans. Comput. Aided Des. Integr. Circuits Syst.*, vol. 38, no. 10, pp. 1811-1819, 2018, Art. no. 18991545.

[7] D. Mamaluy and X. Gao, "The fundamental downscaling limit of field effect transistors," *Appl. Phys. Lett.*, vol. 106, no. 193503, Feb. 2015.

[8] E. Painkras, L. A. Plana, J. Garside, S. Temple, F. Galluppi, C. Patterson, D. R. Lester, A. D. Brown, S. B. Furber, "Spinnaker: A 1-w 18-core system-on-chip for massively-parallel neural network simulation," *IEEE J. Solid-State Circuits*, vol. 48, no. 8, pp. 1943–1953, Aug. 2013, Art. no. 13694053.

[9] P. Ball, "Computer engineering: Feeling the heat," *Nature*, vol. 492, pp. 174-176, Dec. 2012.

[10] I. I. Soloviev, A. E. Schegolev, N. V. Klenov, S. V. Bakurskiy, M. Y. Kupriyanov, M. V. Tereshonok, A. V. Shadrin, V. S. Stolyarov, A. A. Golubov, "Adiabatic superconducting artificial neural network: basic cells," *J. Appl. Phys.*, vol. 124, pp. 152113, Jul. 2018.

[11] H. Katayama, T. Fujii, and N. Hatakeyama, "Theoretical basis of SQUID-based artificial neurons," *J. Appl. Phys.*, vol. 124, no. 152106, Sep. 2018.

[12] R. Cheng, U. S. Goteti, and M. C. Hamilton, "Superconducting neuromorphic computing using quantum phase-slip junctions," *IEEE Trans. Appl. Supercond.*, vol. 29, no. 5, Aug. 2019, Art. no. 1300505.

[13] M. L. Schneider, C. A. Donnelly, I. W. Haygood, A. Wynn, S. E. Russek, M. A. Castellanos-Beltran, P. D. Dresselhaus, P. F. Hopkins, M. R. Pufall and W. H. Rippard, "Synaptic weighting in single flux quantum neuromorphic computing," *Sci. Rep.*, vol. 10, no. 934, Jan. 2020.

[14] E. Toomey, K. Segall, M. Castellani, M. Colangelo, N. Lynch, and K. K. Berggren, "Superconducting nanowire spiking element for neural networks," *Nano. Lett.*, vol. 20, pp. 8059–8066, Sep. 2020.

[15] U. S. Goteti and Robert C. Dynes, "Superconducting neural networks with disordered Josephson junction array synaptic networks and leaky integrate-and-fire loop neurons," *J. Appl. Phys.*, vol. 129, no. 073901, Sep. 2020.

[16] D. H. Ackley and G. E. Hinton, "A learning algorithm for Boltzmann machines," *Cogn. Sci.*, vol. 9, pp. 147-169, Mar. 1985.

[17] J. D. Whitfield, M. Faccin, and J. D. Biamonte, "Ground-state spin logic," *EPL*, vol. 99, no. 57004, Sep. 2012.

[18] Emile H. L. Aarts and Jan H. M. Korst, "Boltzmann machine and their applications," *Lect. Notes Comput. Sci.*, vol. 258, pp. 34- 51, Jun. 1987.

[19] S. C. Smithson, N. Onizawa, B. H. Meyer, W. J. Gross, and T. Hanyu, "Efficient CMOS invertible logic using stochastic computing," *IEEE Trans. Cir. Sys.*, vol. 66, no. 6, pp. 2263-2274, Jan. 2019, Art. no. 18670429.

[20] Y. Lv, R. P. Bloom, and J. P. Wang, "Experimental demonstration of probabilistic spin logic by magnetic tunnel junctions," *IEEE Magn. Lett.*, vol. 10, no. 4510905, Dec. 2019.

[21] J. Biamonte, P. Wittek, N. Pancotti, P. Rebntrost, N. Wiebe, and S. Lloyd, "Quantum machine learning," *Nature*, vol. 549, pp. 195-202, Sep. 2017.

[22] M. H. Amin, E. Andriyash, J. Rolfe, B. Kulchytskyy, and R. Melko, "Qunatum boltzmann machine," *Phys. Rev. X*, vol. 8, no. 021050, May. 2018.

[23] S. Srivastava and V. Sundararaghavan, "Machine learning in quantum computers via general Boltzmann Machines: Generative and Discriminative training through annealing," arXiv:2002.00792, Feb. 2020.

[24] M. Maezawa, G. Fujii, M. Hidaka, K. Imafuku, K. Kikuchi, H. Koike, K. Makise, S. Nagasawa, H. Nakagawa, M. Ukibe, and S. Kawabata, "Toward practical-scale quantum annealing machine for prime factoring," *J. Phys. Soc. Jpn.*, vol. 88, no. 6, Apr. 2019, Art. no. 061012.

[25] N. Takeuchi, Y. Yamanashi, and N. Yoshikawa, "Energy efficiency of adiabatic superconductor logic," *Supercond. Sci. Technol.*, vol. 28, no. 1, Nov. 2014, Art. no. 015003.

[26] S. Bansal, B. Chonigman, C. Puglisi, A. Inamdar, F. Pena, E. Lehmann, S. Gupta, and D. Gupta, "Black-box optimization of superconducting circuits using reduced-complexity neural networks," *IEEE Trans. Appl. Supercond.*, vol. 31, no. 5, Aug. 2021, Art. no. 1400206.

[27] N. Takeuchi, S. Nagasawa, F. China, T. Ando, M. Hidaka, Y. Yamanashi, and N. Yoshikawa, "Adiabatic quantum-flux-parametron cell library designed using a 10 kA cm -2 niobium fabrication process," *Supercond. Sci. Technol.*, vol. 30, no. 3, Mar. 2017, Art. no. 035002.

[28] E. S. Fang and T. Van Duzer, "A Josephson integrated circuit simulator (JSIM) for superconductive electronics application," in Extended Abstracts of *Int. Superconductivity Electronics Conf.*, Tokyo, Japan, 1989, pp. 407–410.

[29] N. Takeuchi, Y. Yamanashi and N.Yoshikawa, "Thermodynamic study of energy dissipation in adiabatic superconductor logic," *Phys. Rev. Appl.*, vol. 4, no. 3, Sep. 2015, Art. no. 034007.

[30] C. J. Fourie, "Full-Gate verification of superconducting integrated circuit layouts with InductEx," *IEEE Trans. Appl. Supercond.*, vol. 25, no. 1, Feb. 2015, Art. no. 1300209.

[31] S. Kullback and R. A. Leibler, "On information and sufficiency," *Ann. Stat.*, vol. 22, pp. 79-86, Mar. 1951.